NASA TM X-637

NASA

TECHNICAL MEMORANDUM

X-637

FLIGHT-SIMULATED OFF-THE-PAD ESCAPE AND LANDING MANEUVERS

FOR A VERTICALLY LAUNCHED HYPERSONIC GLIDER

By Gene J. Matranga, William H. Dana,
and Neil A. Armstrong

Flight Research Center
Edwards, Calif.

NATIONAL AERONAUTICS AND SPACE ADMINISTRATION

WASHINGTON

March 1962

ADC-2445

NATIONAL AERONAUTICS AND SPACE ADMINISTRATION

TECHNICAL MEMORANDUM X-637

FLIGHT-SIMULATED OFF-THE-PAD ESCAPE AND LANDING MANEUVERS

FOR A VERTICALLY LAUNCHED HYPERSONIC GLIDER*

By Gene J. Matranga, William H. Dana,
and Neil A. Armstrong

SUMMARY

A series of subsonic maneuvers simulating typical off-the-pad escape and landing procedures for a vertically launched hypersonic-glider configuration was flown using a delta-wing airplane having a peak effective lift-drag ratio of 4.7.

None of the required maneuvers posed any particularly difficult or taxing situations for the pilots. Circular, overhead landing patterns flown at 240 knots indicated airspeed were relatively easy to perform and resulted in touchdown longitudinal dispersions of less than ±1,200 feet.

A reduction in the pilot's visibility from the cockpit did not noticeably impair his ability to navigate except when view of the area directly beneath the airplane was required. However, portions of the escape and landing maneuvers were adversely affected by the reduced visibility.

INTRODUCTION

From a safety-of-flight standpoint, take-off and landing are, generally, two of the most critical flight control areas. For a hypersonic glider, which is launched vertically from the ground atop a large booster rocket and is landed unpowered, these areas are particularly critical in the event of an emergency prior to launch. One proposal for providing for survival of the pilot and vehicle if a main booster malfunctions on the pad or shortly after lift-off is to propel the vehicle well away from the danger area by means of an auxiliary booster on the vehicle. If the vehicle is boosted high enough and fast enough, the pilot can right the airplane and land on a nearby runway. The problem

*Title, Unclassified.

of landing the glider, however, could be critical, since the lift-drag ratio of several proposed hypersonic-glide configurations is low (about 4), and the vehicle will land unpowered. To further complicate the landing problem, thermal-structural considerations generally dictate that window areas be minimized, thus limiting the pilot's view from the cockpit.

Low-speed X-15 landing maneuvers were successfully simulated in the study reported in reference 1. Based on this program, a series of analytical and flight-simulation studies is being conducted at the NASA Flight Research Center, Edwards, Calif., to investigate the sub-sonic, off-the-pad escape and landing maneuvers of a typical vertically launched hypersonic glider. This paper considers the results of a brief flight-test program in which an attempt was made to match predicted escape and landing maneuvers with flight data. Also considered is the effect on the maneuvers performed of limited pilot visibility from the cockpit.

SYMBOLS

a_n normal acceleration, g units

C_L airplane lift coefficient

g acceleration due to gravity, ft/sec^2

h geometric altitude above touchdown point, ft

$(L/D)'$ effective lift-drag ratio

t time, sec

V true airspeed, ft/sec

$\dot{V}$ derivative of airspeed with time, $\frac{dV}{dt}$, ft/sec^2

V_i indicated airspeed, knots

V_v vertical velocity, ft/sec

x longitudinal distance from touchdown point, ft

y lateral distance from touchdown point, ft

α trim angle of attack, deg

γ flight-path angle, deg

AIRPLANE

The test airplane is a single-place, delta-wing fighter-interceptor powered by a turbojet engine equipped with an afterburner. A three-view drawing and a photograph of the airplane are shown in figures 1 and 2, respectively. The physical characteristics of the airplane are presented in table I.

The wing has an aspect ratio of 2.02 and varies in thickness from 5 percent at the root to 3 percent at the tip. The average wing loading during the tests was 36 lb/sq ft. Speed brakes located on the upper and lower surfaces of the wings were used in conjunction with the landing gear to provide the additional drag required for this investigation.

To further reduce the effective lift-drag ratio, the throttle was modified so that when idle power was selected the afterburner nozzle was forced to the full-open position. This reduced the idle thrust to slightly less than 200 pounds, compared with a normal idle thrust of about 500 pounds.

Longitudinal and lateral control of the airplane are provided by elevons located on the trailing edge of the wing. Directional control is provided by a conventional rudder. Two completely independent hydraulic systems operate the outboard elevons. The inboard elevons are electrically slaved to the outboard elevons and are actuated by electrohydraulic valves. Longitudinal-control forces are supplied artificially by a bungee and bobweight combination and are programed as a function of Mach number. Lateral-control forces are supplied artificially by a bungee. The rudder is operated by a hydraulically powered system providing no external force feedback. Pedal forces are supplied artificially with a bungee. No artificial damping was provided during any of the maneuvers performed in this investigation.

INSTRUMENTATION

No internal recording instruments were used during the tests. All flight data presented were obtained from Air Force Flight Test Center Askania cinetheodolite cameras operating at 1 frame per second. Three-station solutions of these data determined the airplane position in space at any time. By differentiating the position data, forward velocity and vertical velocity were obtained. From a knowledge of airplane forward velocity, altitude, and wind conditions, indicated airspeeds were determined.

TESTS

Before attempting any simulated landing or off-the-pad escape maneuvers, a series of constant-speed, wings-level glides was performed to ascertain the lift-drag-ratio variation with airspeed. Tests were made at several engine power settings with only the gear extended and with the gear and the speed brakes extended. For most of the maneuvers discussed, the configuration consisted of gear and speed brakes in the extended position and engine at idle power with the afterburner nozzle open.

The escape maneuvers were entered into by executing a high-speed run about 1,000 feet above the ground in the clean configuration. At a predetermined point, the pilot performed a pull-up. At the vertical-attitude position, engine power was reduced to idle and the speed brakes were extended. This position corresponds to glider auxiliary-booster-rocket burnout and is where the simulation begins. As the pull-over continued, the gear was extended at the gear-extension-limit speed (260 KIAS). When the inverted, horizontal position was attained, the pilot rolled the vehicle to the erect, level attitude, accelerated to approach speed, and landed. Figure 3 aids in visualizing the relation between this maneuver and the escape maneuver of a vertically launched vehicle. This perspective sketch shows that the two trajectories merge when the test airplane reaches the vertical attitude and when the glider's booster rocket burns out; succeeding portions of the trajectories are coincident. It should be noted that two different speeds were utilized in the high-speed run, resulting in different speed and altitude combinations at the vertical attitude, thereby simulating a variety of auxiliary-booster-rocket capabilities.

To simulate the approach and landing maneuvers, a series of 360°-spiral, overhead landing patterns was performed at speeds from 180 KIAS to 290 KIAS and bank angles from 30° to 60°. Several straight-in landing patterns were also performed at about 240 KIAS. All landings executed by the five participating pilots were made on the lakebed of Rogers Dry Lake at Edwards Air Force Base, Calif.

During most of the tests, the airplane canopy was fitted with an amber Plexiglas mask cut out to provide the pilot with a field of vision comparable to that of a currently proposed boost-glide vehicle. The pilot, with a blue visor in place, could see only through the cut-out portions of the mask. With the visor raised, the pilot could utilize the full field of view of the test aircraft.

RESULTS AND DISCUSSION

For convenience of presentation, the results of the various phases of this investigation are treated individually in the following discussion. First, the ranges of lift-drag ratios and angles of attack utilized are noted and compared with corresponding values anticipated for some hypersonic-glider vehicles. Succeeding subsections consider the off-the-pad escape maneuver; the landing, both following escape and during normal operations; the flare and touchdown; and the pilot's evaluation of the influence of cockpit visibility on his performance of the various maneuvers. Because of the lack of on-board instrumentation and the importance of qualitative evaluation in the critical flight areas being studied, pilot comments are relied upon heavily throughout this paper.

Glider Performance

The variations of angle of attack and effective lift-drag ratio with lift coefficient for the test airplane with the gear and the speed brakes extended, the engine at idle power setting, and the afterburner nozzle open are presented in figure 4. The angle-of-attack data were obtained from unpublished reports of the manufacturer's flight tests. The effective lift-drag ratios were determined from data obtained during constant-speed glides from an altitude of 20,000 feet to 5,000 feet by utilizing the forward speed and the rate of descent to determine the glide angle γ. Also, the rate of change of true airspeed was readily calculated, since the pilot flew a constant indicated airspeed during the approaches. These quantities were then combined in the following equation to obtain the effective lift-drag ratio

$$(L/D)' = \frac{g}{g \tan \gamma - \dot{V}}$$

The average lift coefficient was determined as a function of wing loading and the average dynamic pressure in the glides.

The faired data of figure 4 show that the peak lift-drag ratio of 4.7 occurred at a lift coefficient of 0.38 and an angle of attack of about 10°.

The trim angle-of-attack and effective lift-drag-ratio data from figure 4 are presented in figure 5 as a function of indicated airspeed at a wing loading of 36 lb/sq ft. For comparison, similar data for a proposed boost-glide vehicle at a wing loading of 28 lb/sq ft are

included. The data for the two configurations are in good agreement, which indicates that the test airplane should closely simulate the performance of the proposed vehicle. In fact, the comparison is better than achieved in the successful simulation of the X-15 airplane discussed in reference 1.

Off-the-Pad Escape Maneuver

More than 40 simulated off-the-pad escape maneuvers were accomplished during this phase of the study. The maneuver is preceded by a low-altitude, high-speed run followed by a pull-up to a vertical attitude. At this point, power is reduced to idle and the speed brakes are extended. The pull-over is continued, and the landing gear is lowered at approximately 260 KIAS. When a horizontal, but inverted, attitude is reached, the pilot rolls to the erect, level attitude and accelerates to the proper approach speed.

Two sets of conditions exemplifying typical auxiliary-boost-rocket capabilities were considered. Figure 6 presents a typical trajectory of a high-energy escape and landing maneuver, and figure 7 presents a time history of the escape phase only. From an initial airspeed of about 500 KIAS during the low-level run, a 3.5g pull-up is performed. The vertical attitude is reached at an altitude of about 10,000 feet with a speed of less than 400 KIAS. With the pull-over continued at a reduced normal acceleration (approx. 2g), the peak altitude of 14,300 feet was realized with a speed of 172 KIAS about 32 seconds after the initiation of the maneuver. The approach pattern was flown at 240 KIAS with an average bank angle of 30°.

The trajectory and time history of a low-energy maneuver are presented in figures 8 and 9, respectively. With an initial speed of about 400 KIAS and a 4.5g pull-up, the airplane reaches the vertical attitude at an altitude of about 5,000 feet with a speed of about 320 KIAS. Normal acceleration is again reduced to about 2g, and the airplane goes "over the top" at an altitude of about 8,000 feet and an airspeed of 150 KIAS. Although the approach pattern shown in figure 8 is flown at 240 KIAS, it is considered to be a much tighter pattern than that of figure 6 because of the lower initial altitude on the downwind leg of the pattern. There is also much less margin for error, since little excess altitude is available anywhere around the pattern.

The following tabulation summarizes the average conditions for the more than 40 maneuvers performed:

Entry		Pull-up	Simulated burnout point		Pull-over	Over-the-top	
V_i, knots	h, ft	a_n, g	V_i, knots	h, ft	a_n, g	V_i, knots	h, ft
525	1,000	3.5	400	9,500	≈ 2.0	190	15,000
400	1,000	4.5	325	5,000	≈ 2.0	155	8,000

The pilots reported that the escape maneuvers, as performed in this investigation, were not particularly difficult or taxing and showed no significant difference in handling characteristics between the two types of maneuvers flown. This opinion is based upon the ability of the pilot to place the airplane on the downwind leg of the pattern at a more precise position and energy level in the escape maneuvers than is normally attained in power-off approaches.

Landing Patterns

In addition to the landings performed after each escape maneuver, a series of power-off landing approaches was performed over a speed range from 180 KIAS to 290 KIAS. Straight-in approaches as well as 360°-spiral, overhead patterns using from 30° to 60° of bank angle were made.

In these approaches it is most significant that the pilot was consistently able to position the aircraft at the approach end of the runway at the proper landing speed. Also, all five participating pilots agreed that a circular, overhead pattern similar to that shown in figure 10 was easiest and most comfortable because it afforded a proper balance of excess energy without an excessively large rate of descent. This pattern (fig. 10), flown at 240 KIAS with a bank angle between 30° and 40°, is entered at a high-key altitude of about 15,000 feet. The average radius of turn was about 7,000 feet and resulted in a downwind-leg altitude of 8,000 feet and a base-leg altitude of 3,500 feet. The average rate of sink in this pattern was about 120 ft/sec, and the peak rate was about 140 ft/sec.

In particular, these landing tests showed that, with an altitude of 7,000 feet and a lateral displacement of 2.5 nautical miles on the downwind leg of the pattern (as with the lower-energy off-the-pad escape maneuvers), some indications of the limitations of the pattern

could be determined. A velocity of 240 KIAS was flown in the patterns so that sufficient energy would be available to successfully execute the flare and touchdown. The combinations of geographic boundary conditions and minimum flying speed required that a bank angle of about 30° be utilized. Any further increase in speed would require increased bank angles with reduced transit times and increased pilot response, thereby making the maneuver more taxing for the pilot.

As in the tests of reference 2, the pilots found that the slower approach speeds and sink rates associated with a wing loading of 30 lb/sq ft to 40 lb/sq ft resulted in more comfortable patterns than experienced in similar tests (ref. 3) using a vehicle with a wing loading near 80 lb/sq ft.

H
2
7
5

Flare and Touchdown

The advantages of low wing loading are particularly evident in the execution of the flare. The slow approach speeds and low rates of descent available with a low-wing-loading vehicle allow the pilot to delay the flare to a lower range of altitudes where he can more accurately judge his position. The change of flight path during the flare was definite and the rate of loss of airspeed during the flare was small enough to allow the pilot to take corrective action without decelerating to a dangerously low speed.

The time history of a typical flare maneuver is presented in figure 11. The flare-initiation speed was 235 KIAS, and the altitude was about 500 feet. At the completion of the flare, the speed diminished to 205 KIAS. At this point, approximately 10 seconds remained for the final glide and deceleration to touchdown at a speed of 174 KIAS. During this final floating phase, no additional drag could be added to the test airplane to simulate the gear extension on the hypersonic vehicle. However, even if average speed bleed-off of 3 knots/second to 4 knots/second could have been doubled in these tests, the test airplane would be in a class with the X-15 (see ref. 1), and the touchdown maneuver still would not be critical.

The average touchdown speed during these tests was about 170 KIAS. The rate of sink at touchdown was less than 3 ft/sec and averaged about 2 ft/sec. Touchdown longitudinal dispersions ranged between ±1,200 feet of the intended touchdown point, which is similar to that measured with the X-15 airplane (ref. 1).

Pilot Vision-Field Simulation

During a portion of these maneuvers, the test-airplane canopy was restricted to give the pilot a field of view comparable to that anticipated for a currently proposed boost-glide vehicle. Figure 12 is an illustration of the airplane canopy fitted with two different amber Plexiglas masks. With a blue visor in place, the pilot could see only through cut-out portions of the mask; however, with the visor raised, the pilot was free to utilize the view field normally available from the test aircraft.

The restriction of vision did not noticeably reduce the pilot's high-altitude-navigation capability except when it was necessary to locate some geographical landmark directly beneath the aircraft. The restricted vision did cause considerable difficulty because of the lack of a horizon reference during the portion of the escape maneuver from the vertical-attitude position to the point where the horizon reappeared. This segment of 3 to 4 seconds extended through approximately 45° of rotation in pitch. Once the horizon appeared during the pull-over, the restricted vision posed no added hardship, however. It was noticed that the amber Plexiglas without the visor lowered was sufficiently restrictive to cause a noticeable deterioration in the quality of the maneuver.

Location of the high-key point was difficult with the restricted visibility, since the vehicle passed directly over this point. Other difficulties were encountered on the downwind leg of the approach pattern where lateral vision was insufficient, and during the 135° to 45° segment prior to rollout of the tight patterns where a view through the masked corner of the canopy was desired. Otherwise, vision was adequate after the aircraft had arrived within 45° of the runway heading on the final approach and remained adequate throughout the flare and landing.

CONCLUSIONS

A delta-wing airplane having a maximum effective lift-drag ratio of 4.7 was used to perform a series of subsonic, flight-simulated off-the-pad escape and landing maneuvers of a vertically launched hypersonic glider. From this study the following conclusions can be made:

1. The off-the-pad escape maneuvers were not considered difficult or taxing by the pilot and were such that the pilot could position the airplane on the downwind leg more precisely than he could in normal power-off approaches.

2. After performing a series of straight-in and circular, overhead approaches, the pilots concluded that a circular pattern flown at 240 knots indicated airspeed was most desirable.

3. The flare maneuver was easy to judge and control. The touchdown longitudinal dispersions could be kept within ±1,200 feet without exceeding a touchdown rate of descent of 3 feet per second.

4. A reduction in the pilot's visibility from the cockpit did not noticeably decrease his high-altitude-navigation capability except when it was necessary to observe the terrain directly beneath the aircraft. However, portions of the off-the-pad escape maneuver and landing approaches were adversely affected.

Flight Research Center,
    National Aeronautics and Space Administration,
        Edwards, Calif., January 22, 1962.

H
2
7
5

REFERENCES

1. Matranga, Gene J.: Analysis of X-15 Landing Approach and Flare Characteristics Determined From the First 30 Flights. NASA TN D-1057, 1961.

2. Matranga, Gene J., and Menard, Joseph A.: Approach and Landing Investigation at Lift-Drag Ratios of 3 to 4 Utilizing a Delta-Wing Interceptor Airplane. NASA TM X-125, 1959.

3. Matranga, Gene J., and Armstrong, Neil A.: Approach and Landing Investigation at Lift-Drag Ratios of 2 to 4 Utilizing a Straight-Wing Fighter Airplane. NASA TM X-31, 1959.

TABLE I.- PHYSICAL CHARACTERISTICS OF THE TEST AIRPLANE

Wing:
    Airfoil section, root . . . . NACA 0005-1.1-30-6° (Modified)
    Airfoil section, tip . . . . NACA 0003-1.1-30-6° (Modified)
    Area, sq ft 557
    Span, ft 33.50
    Mean aerodynamic chord, ft 18.25
    Root chord, ft 25.08
    Tip chord, ft 8.33
    Aspect ratio 2.02
    Taper ratio 33
    Sweep at leading edge, deg 52.50
    Sweep at quarter chord, deg 46.50
    Sweep at trailing edge, deg 16.50
    Incidence, deg 0
    Dihedral, deg 0
    Geometric twist, deg 0

Outboard elevon:
    Area (per side), sq ft 24.26
    Span (normal to fuselage reference line), ft 11.73
    Mean aerodynamic chord, ft 2.04
    Maximum deflection, up, deg 40
    Maximum deflection, down, deg 20

Inboard elevon:
    Area (per side), sq ft 9.04
    Span (normal to fuselage reference line), ft 2.58
    Mean aerodynamic chord, ft 3.75
    Maximum deflection, up, deg 30
    Maximum deflection, down, deg 5

Slat:
    Area (per side), sq ft 7.96
    Span, ft 4.56
    Mean aerodynamic chord, ft 1.10
    Slat chord/wing chord 13

Vertical tail:
    Airfoil section, root . . . . NACA 0005-1.1-25-6° (Modified)
    Airfoil section, tip . . . . NACA 0003.2-1.1-50-6° (Modified)
    Area, sq ft 69.87
    Span, ft 9.46
    Mean aerodynamic chord, ft 7.85
    Aspect ratio 1.28
    Taper ratio 46
    Sweepback of quarter chord, deg 48.22

Rudder:
    Area, sq ft 9.29
    Span (normal to fuselage reference line), ft 6.26
    Mean aerodynamic chord, ft 1.23

Upper-wing speed brakes:
    Area (per side), sq ft 3.26
    Span, ft 2.38
    Maximum deflection, deg 45

Lower-wing speed brakes:
    Area (per side), sq ft 3.26
    Span, ft 2.38
    Maximum deflection, deg 60

Fuselage:
    Frontal area, sq ft 18.70
    Length, ft 53.80
    Fineness ratio 7.86
    Wetted area, sq ft 466

Test center-of-gravity location, percent mean aerodynamic chord 23

Weight:
    Gross, lb 26,100
    Empty, lb 17,100
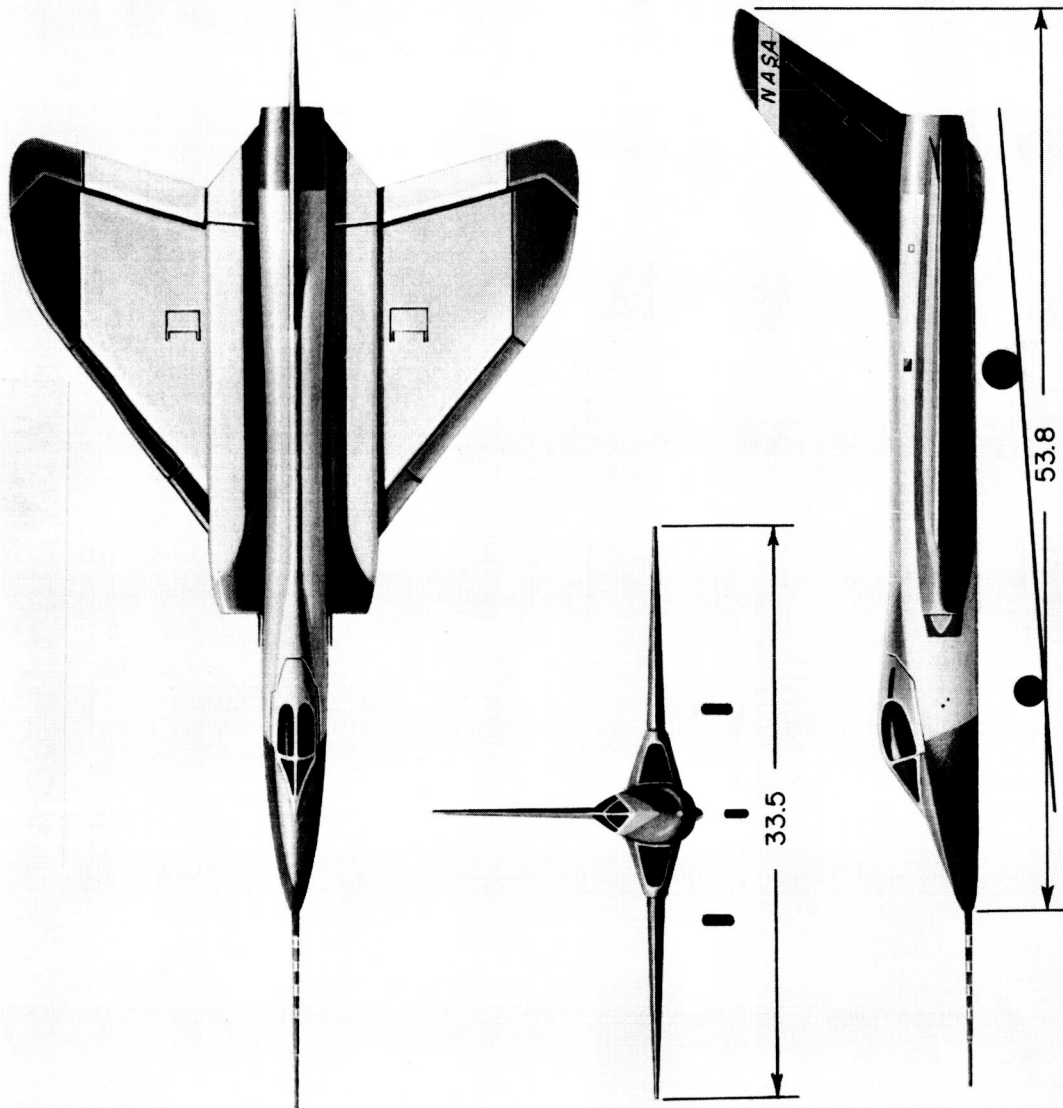
Figure 1.- Three-view drawing of the test airplane. All dimensions in feet.
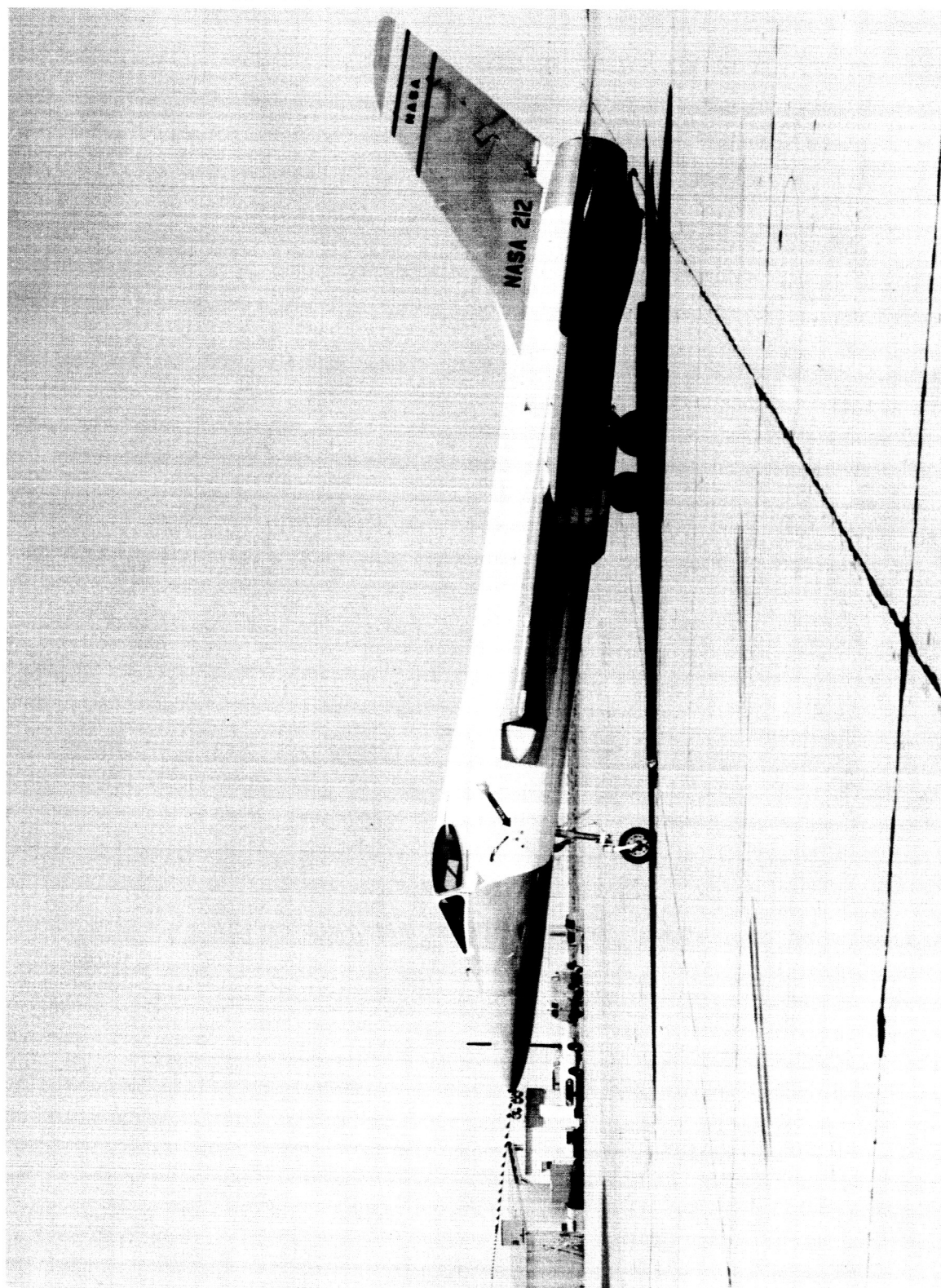
H-275

53.8

33.5

NASA

Figure 2.- Photograph of the test airplane.
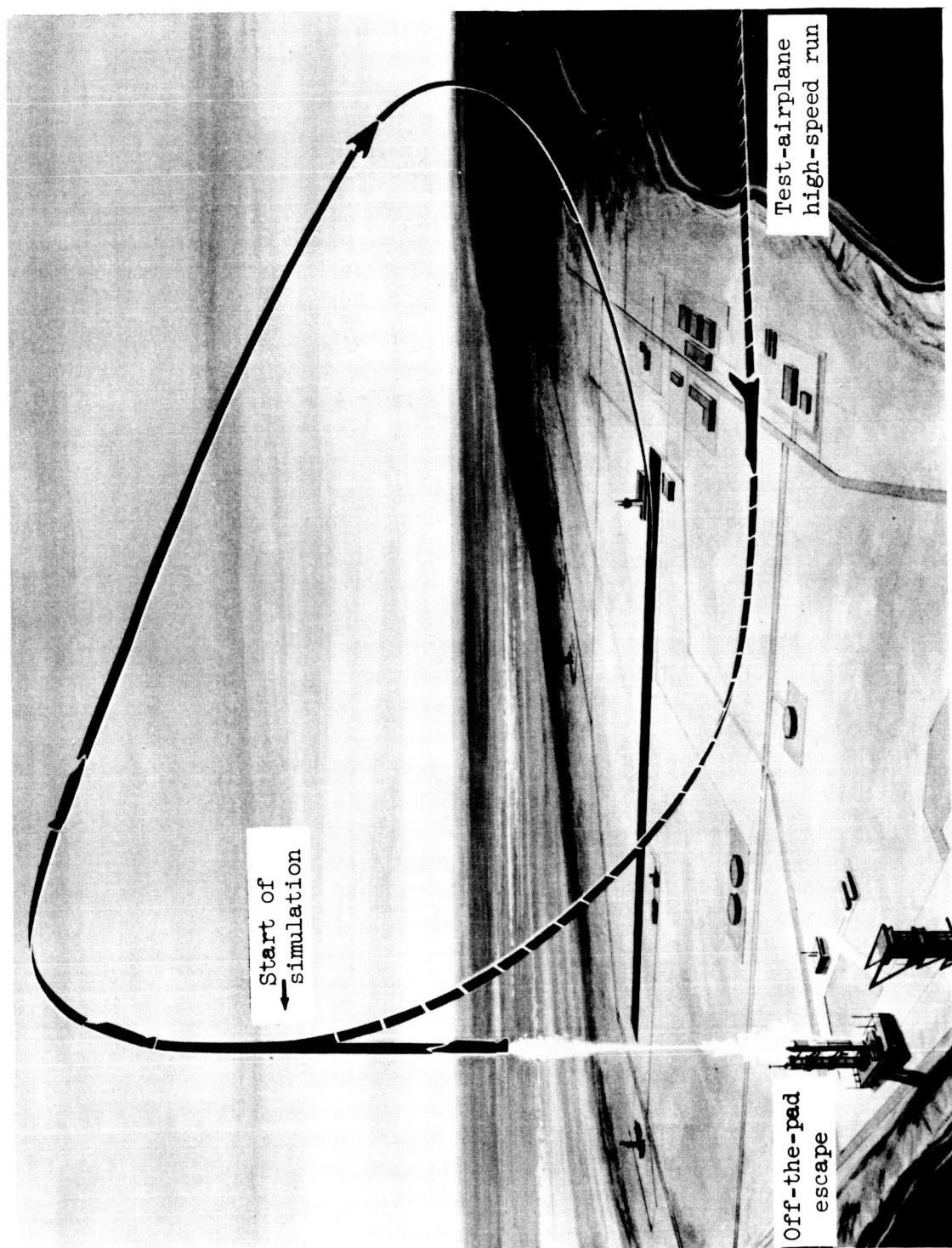
Figure 3.- Perspective drawing of test-airplane maneuver superimposed on hypersonic glider off-the-pad escape and landing maneuver.
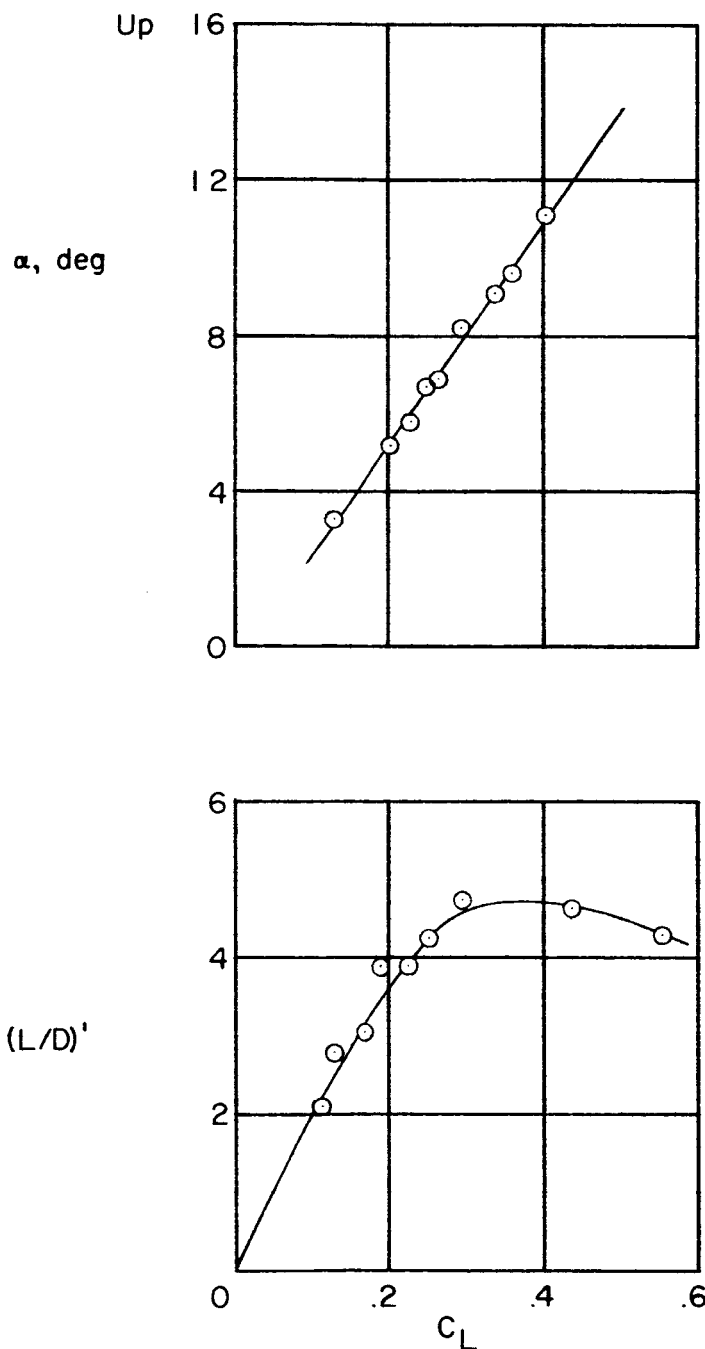
E-7598

H-275

Figure 4.- Trim angle of attack and effective lift-drag ratio as a function of lift coefficient for the test airplane. Gear and speed brakes extended; engine at idle power with afterburner nozzle open.
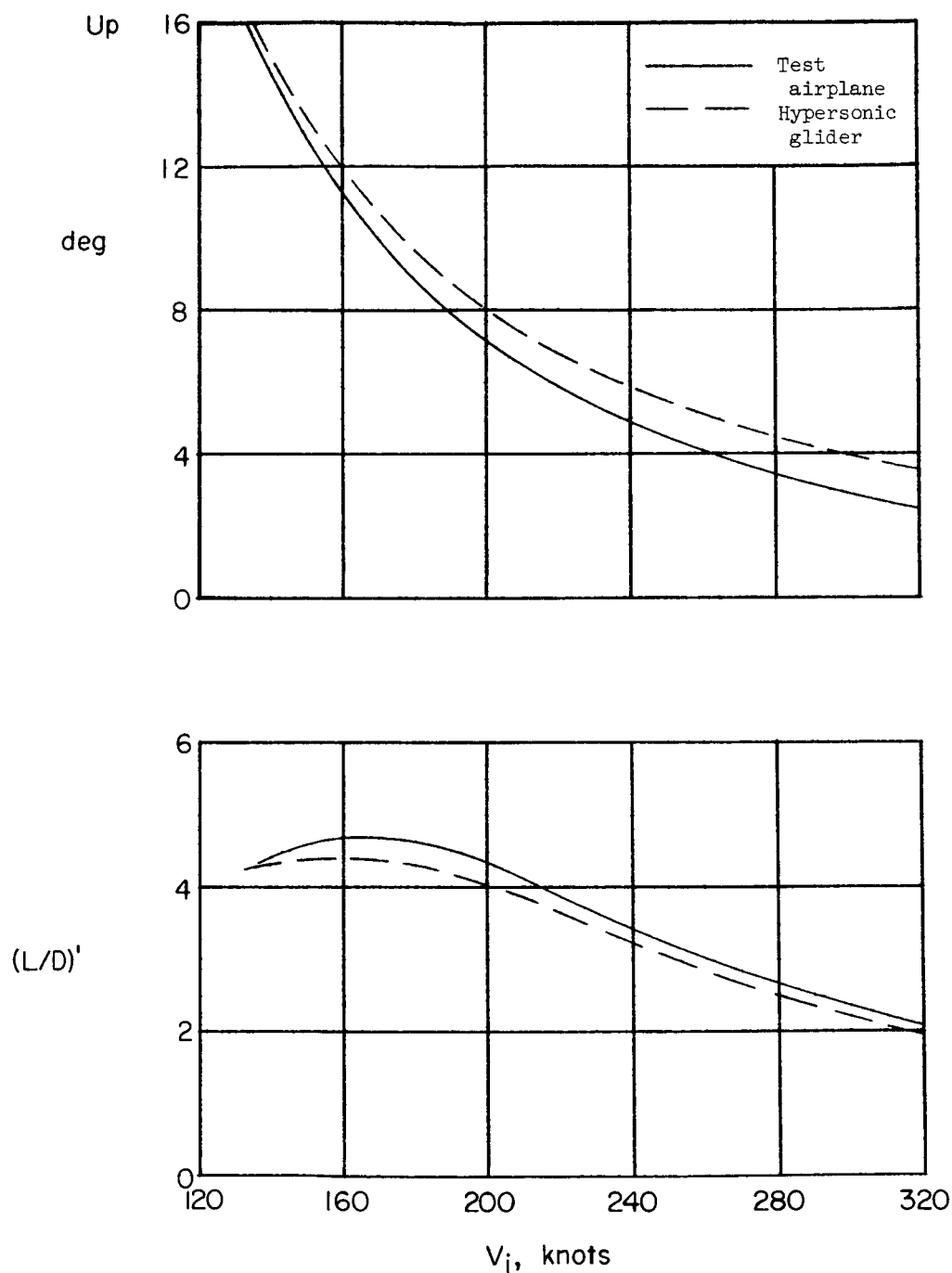
Figure 5.- Trim angle of attack and effective lift-drag ratio as a function of indicated airspeed for the test airplane with a wing loading of 36 lb/sq ft and the boost-glide vehicle with a wing loading of 28 lb/sq ft.
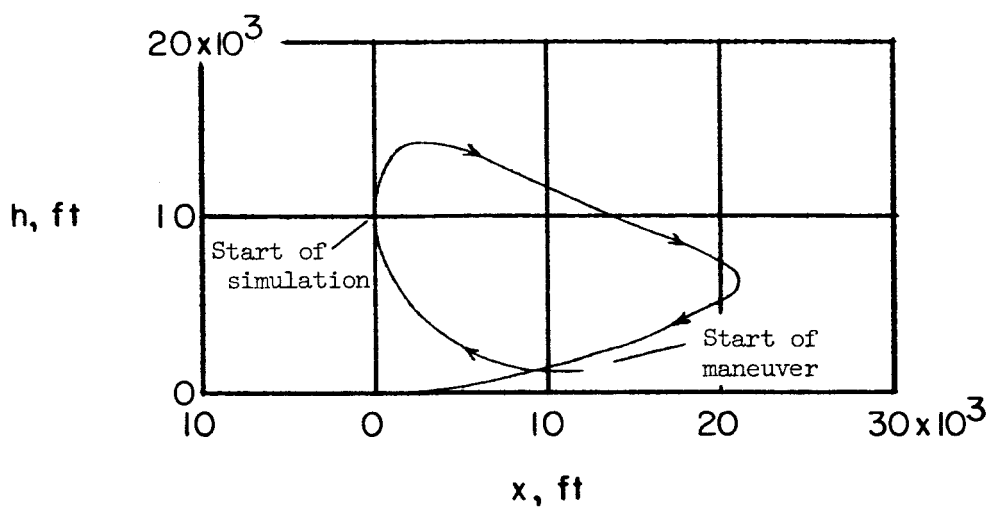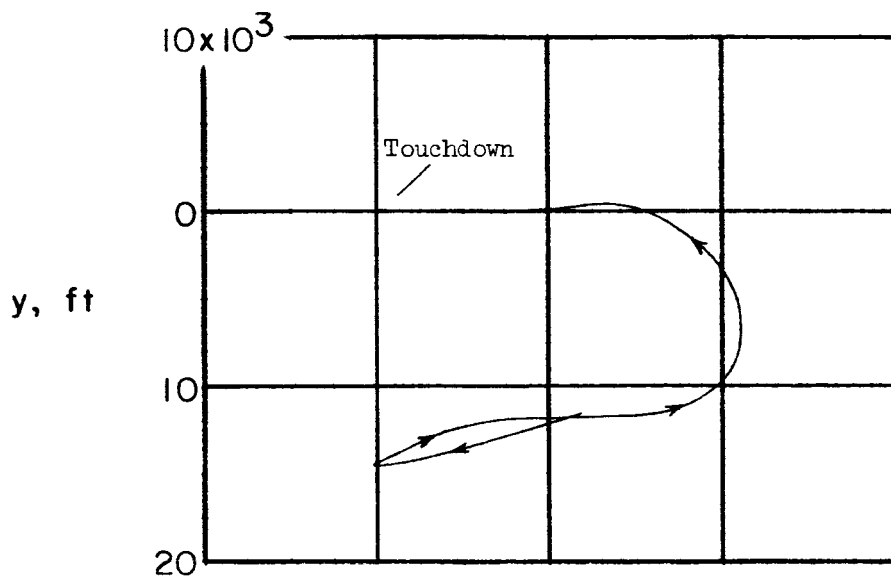
Figure 6.- Trajectory of typical high-energy off-the-pad escape and landing maneuver. Initial $V_i \approx 500$ KIAS; glide $V_i \approx 240$ KIAS.
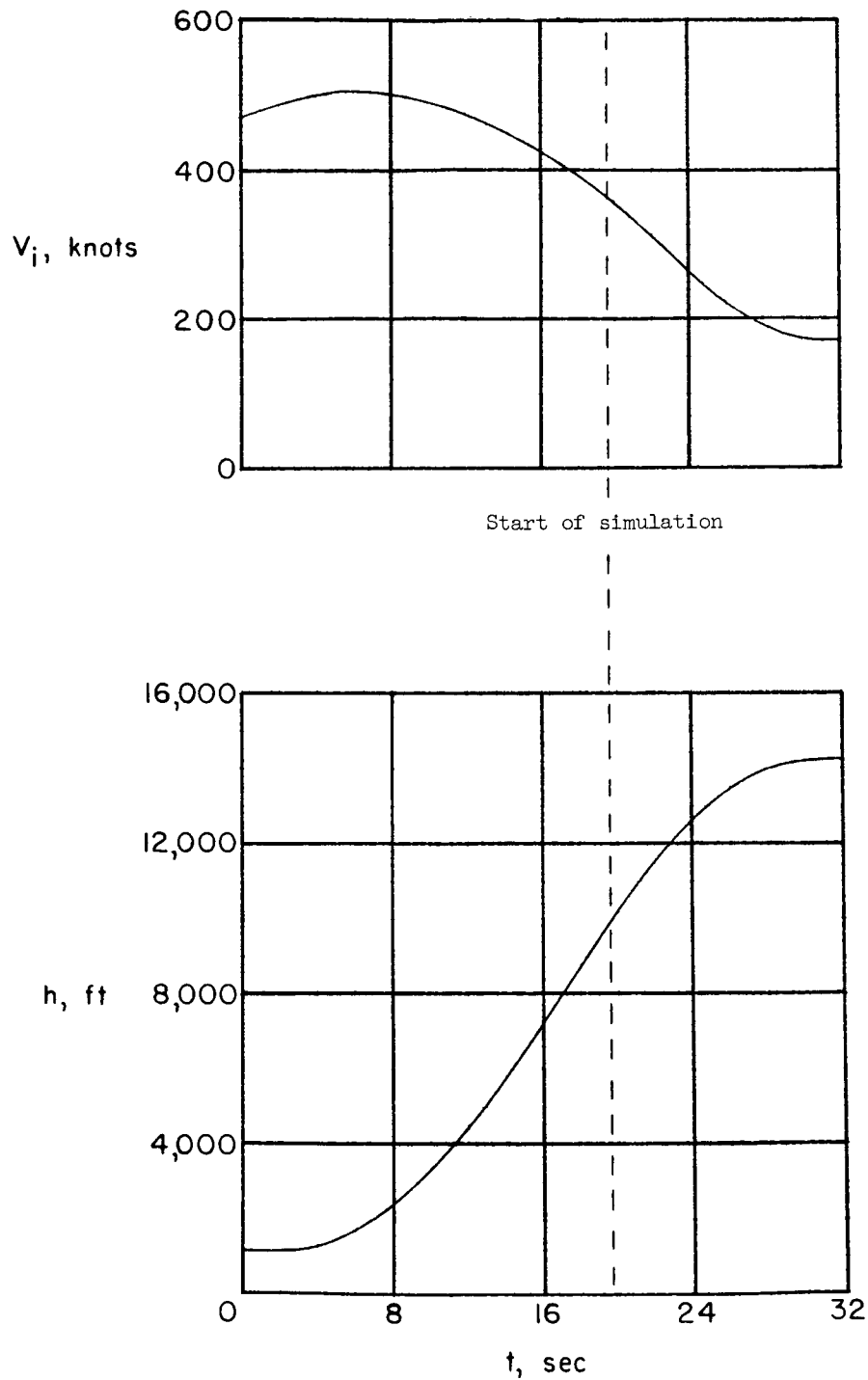
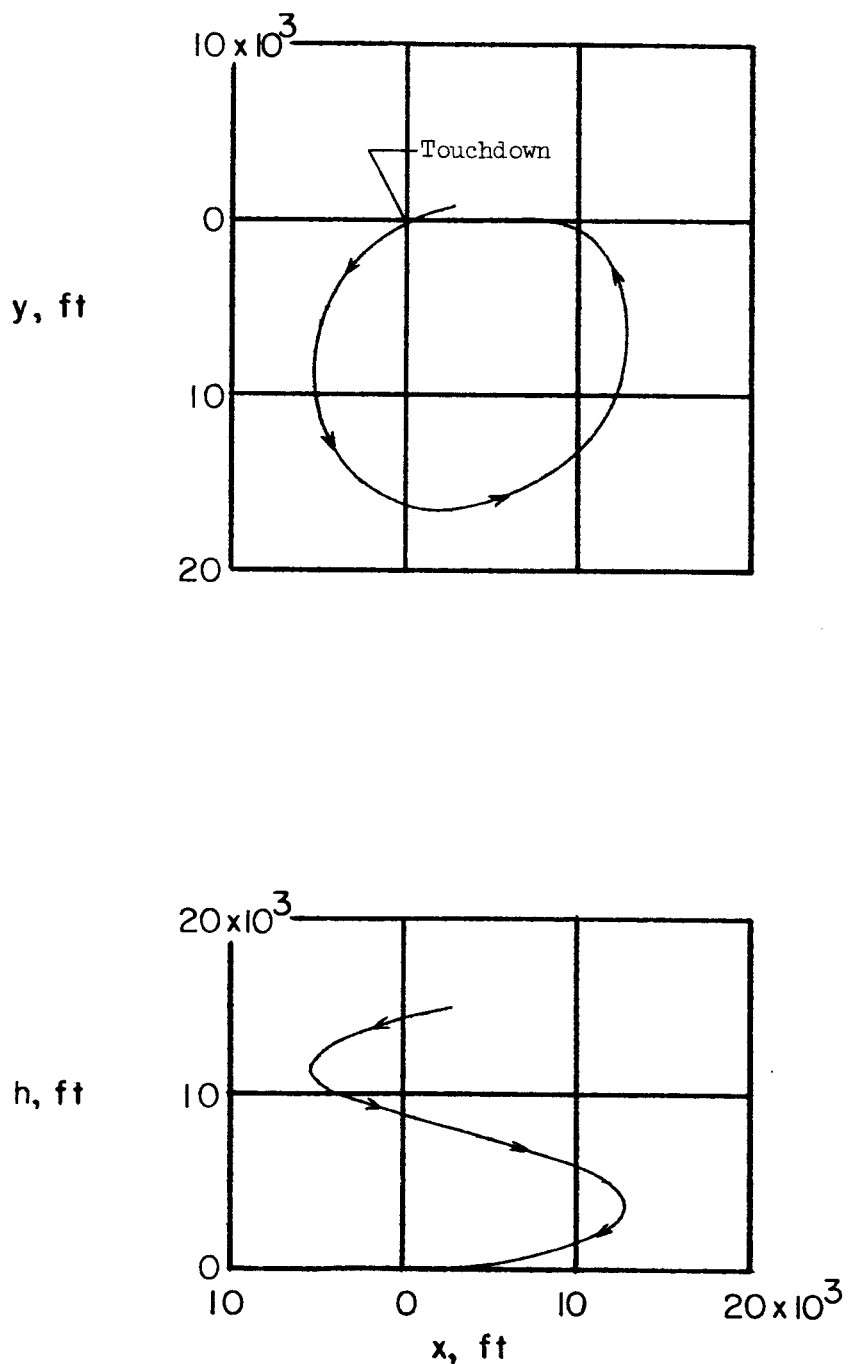Figure 7.- Time history of typical high-energy off-the-pad escape maneuver.

H-275
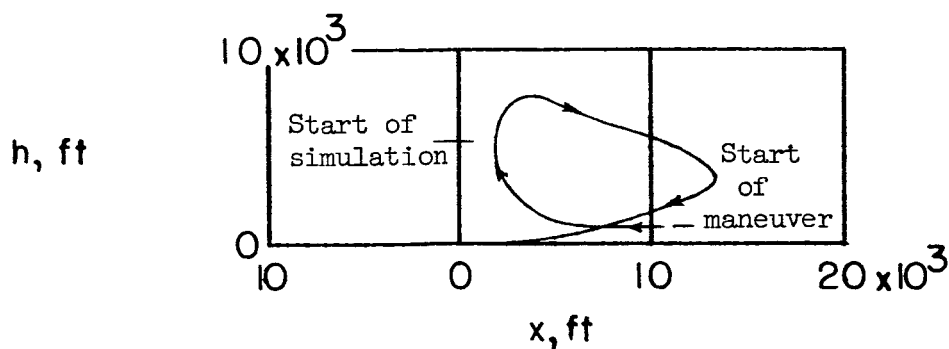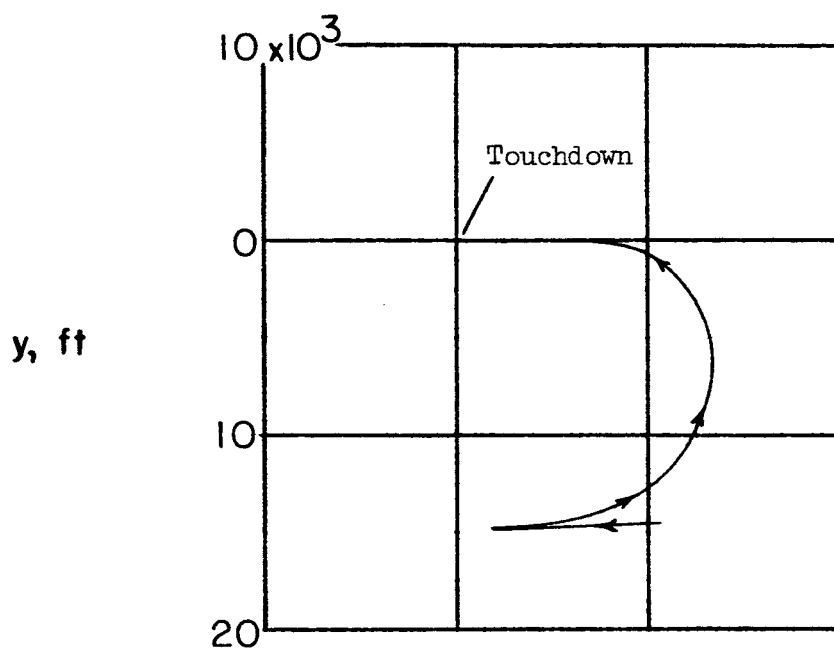
Figure 8.- Trajectory of typical low-energy off-the-pad escape and landing maneuver. Initial $V_i \approx 400$ KIAS; glide $V_i \approx 240$ KIAS.
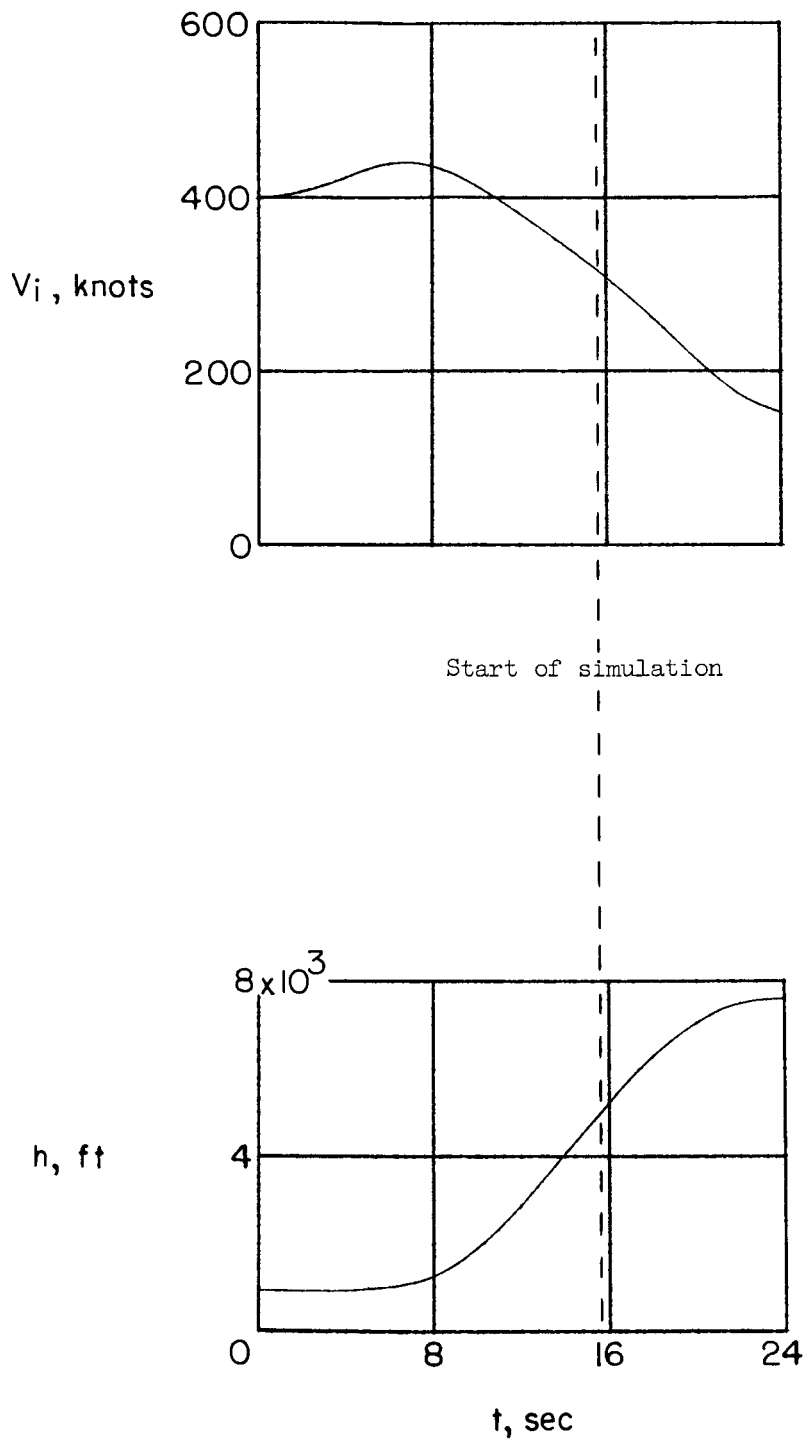
Figure 9.- Time history of typical low-energy off-the-pad escape maneuver.

H-275

Figure 10.- Typical landing pattern. $V_i \approx 240$ KIAS; angle of bank $\approx 30°$; gear and speed brakes extended and engine at idle power with after-burner nozzle open.
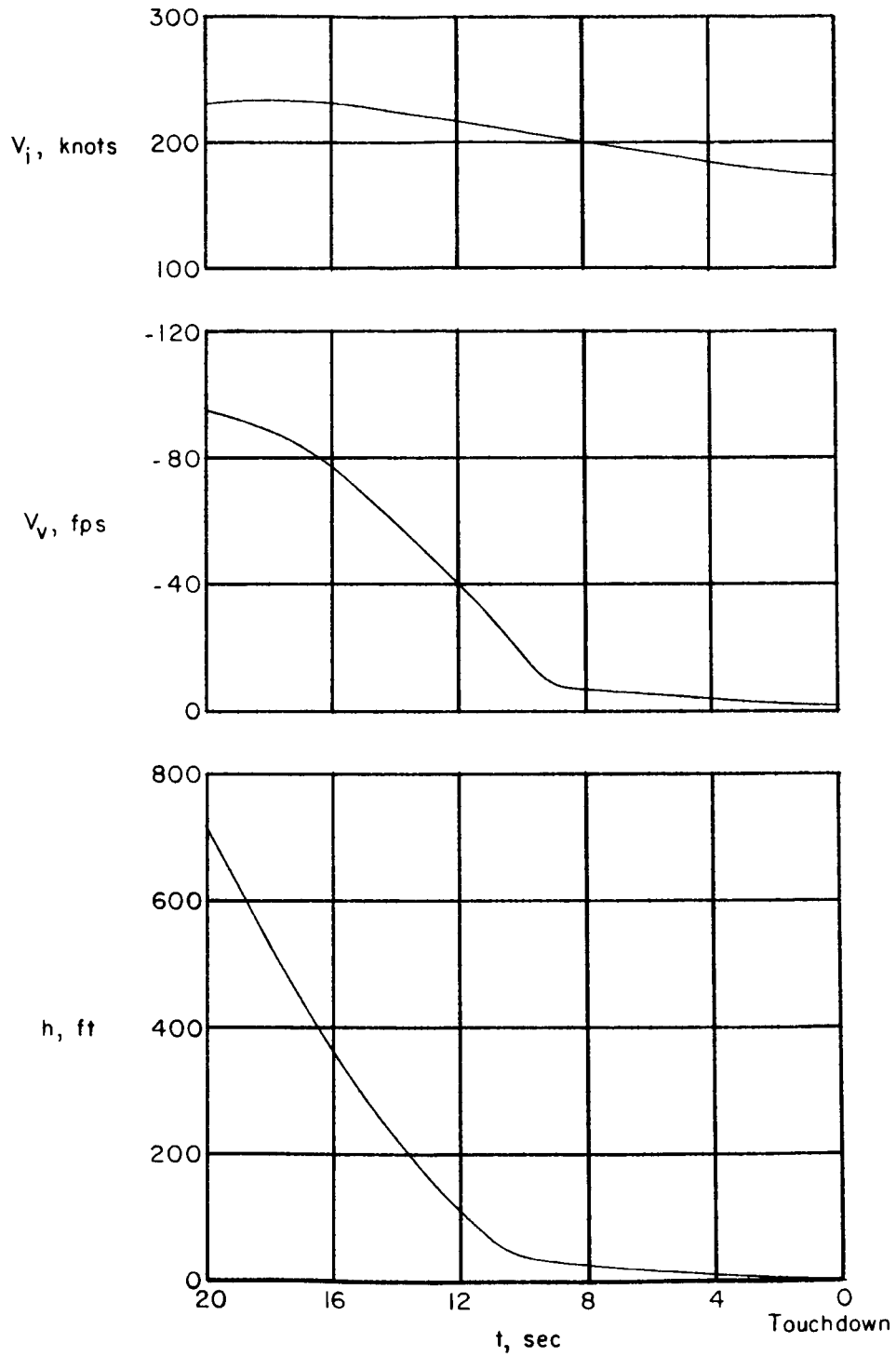
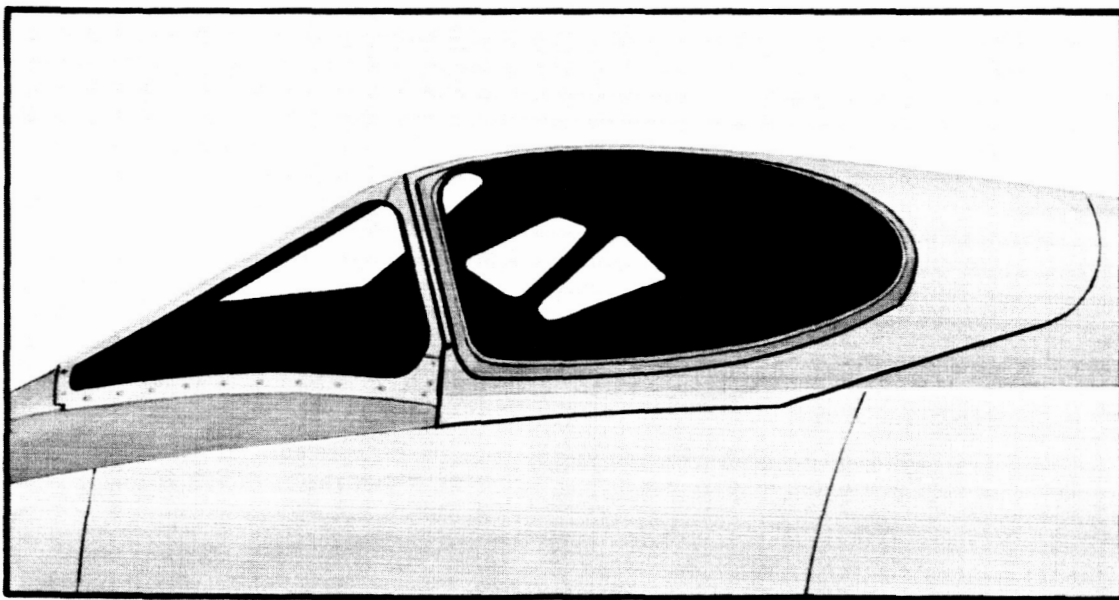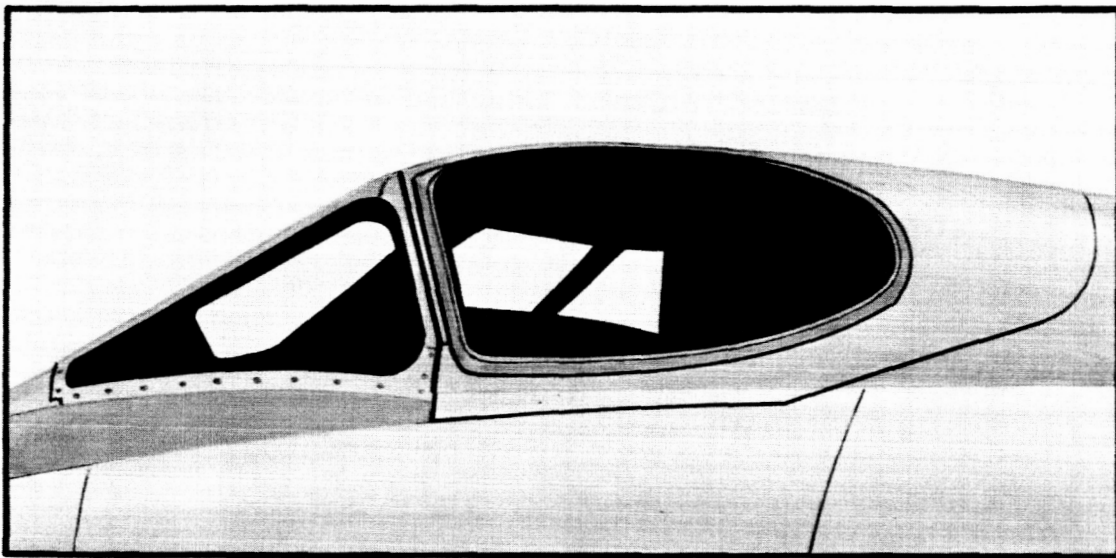Figure 11.- Time history of typical flare maneuver.

H-275

Figure 12.- Illustration of airplane canopy fitted with two different
amber Plexiglas masks.